frontiers in Chemistry

ORIGINAL RESEARCH
published: 12 November 2021
doi: 10.3389/fchem.2021.796695

Ab Initio Calculations for the Electronic, Interfacial and Optical Properties of Two-Dimensional AlN/Zr_2CO_2 Heterostructure

Kai Ren[1†], *Ruxin Zheng*[1†], *Junbin Lou*[2], *Jin Yu*[3], *Qingyun Sun*[1*] *and Jianping Li*[4*]

[1]School of Mechanical and Electronic Engineering, Nanjing Forestry University, Nanjing, China, [2]School of Information Science and Engineering, Jiaxing University, Jiaxing, China, [3]School of Materials Science and Engineering, Southeast University, Nanjing, China, [4]School of Automotive and Transportation Engineering, Shenzhen Polytechnic, Shenzhen, China

OPEN ACCESS

Edited by:
Zhaofu Zhang,
University of Cambridge,
United Kingdom

Reviewed by:
Chao Zhang,
Anhui University of Science and Technology, China
Huasong Qin,
Xi'an Jiaotong University, China

***Correspondence:**
Jianping Li
szyljp0170@szpt.edu.cn
Qingyun Sun
sunqingyun@njfu.edu.cn

[†]These authors have contributed equally to this work and share first authorship

Specialty section:
This article was submitted to Theoretical and Computational Chemistry, a section of the journal Frontiers in Chemistry

Received: 17 October 2021
Accepted: 25 October 2021
Published: 12 November 2021

Citation:
Ren K, Zheng R, Lou J, Yu J, Sun Q and Li J (2021) Ab Initio Calculations for the Electronic, Interfacial and Optical Properties of Two-Dimensional AlN/Zr_2CO_2 Heterostructure. Front. Chem. 9:796695. doi: 10.3389/fchem.2021.796695

Recently, expanding the applications of two-dimensional (2D) materials by constructing van der Waals (vdW) heterostructures has become very popular. In this work, the structural, electronic and optical absorption performances of the heterostructure based on AlN and Zr_2CO_2 monolayers are studied by first-principles simulation. It is found that AlN/Zr_2CO_2 heterostructure is a semiconductor with a band gap of 1.790 eV. In the meanwhile, a type-I band structure is constructed in AlN/Zr_2CO_2 heterostructure, which can provide a potential application of light emitting devices. The electron transfer between AlN and Zr_2CO_2 monolayer is calculated as 0.1603 |e| in the heterostructure, and the potential of AlN/Zr_2CO_2 heterostructure decreased by 0.663 eV from AlN layer to Zr_2CO_2 layer. Beisdes, the AlN/Zr_2CO_2 vdW heterostructure possesses excellent light absorption ability of in visible light region. Our research provides a theoretical guidance for the designing of advanced functional heterostructures.

Keywords: first-principles calculation, AlN/Zr_2CO_2, type-I band alignment, applications, heterostructure

INTRODUCTION

In 2004, the graphene was prepared and discovered to possess abundant interesting performances (Geim and Novoselov, 2007), which has also encouraged researchers to explore other two-dimensional (2D) materials (Pumera and Sofer, 2017; Sun et al., 2020a; Wang et al., 2020a; Sun and Schwingenschlögl, 2020; Zhang et al., 2021a; Tan et al., 2021) different with bulk materials (Chen et al., 2021). These 2D materials have attracted much attentions because of their unique electronic (Qi et al., 2020), magnetic (Wang et al., 2020b), thermal (Xie et al., 2014; Qin et al., 2019a), mechanical (Qin and Liu, 2017) and optical properties (Wang et al., 2020c). For example, at room temperature, black phosphorus with a thickness of less than 7.5 nm can display transistor performance, and the leakage current modulation order is 10^5 (Li et al., 2014). Arsenene can adjust its band gap by applying external strain on the surface (Kamal and Ezawa, 2015). Based on transition-metal dichalcogenides (TMDs), PtS_2, the mobility of field effect transistors (FETs) has been proved to be at least 200 $cm^2/V{\cdot}s$ (Pi et al., 2019). All those desirable characteristics promise 2D materials in future advanced applications, such as, photocatalyst (Wang et al., 2019; Zhang et al., 2020a), metal-ion batteries (Sun and Schwingenschlögl, 2021a), and photoelectric devices (Zhang et al., 2020b; Lou et al., 2021).

Recently, in order to further extend the performance and application range of these 2D materials, the prediction of new 2D materials (Sun et al., 2020b; Ding et al., 2020; Sun and Schwingenschlögl,

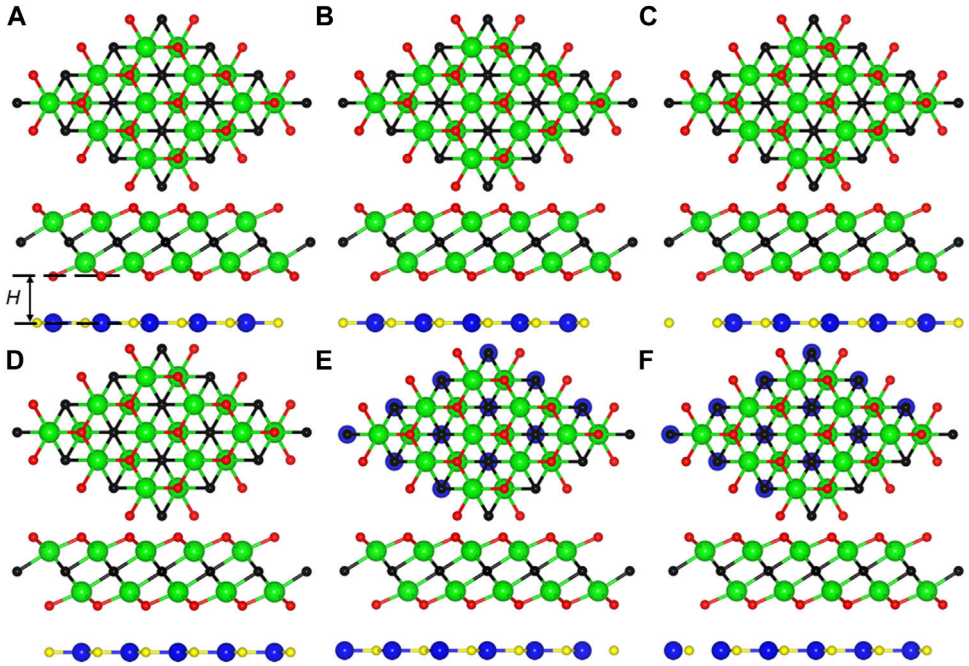

FIGURE 1 | The top and side views of the **(A)** AO-1, **(B)** AO-2, **(C)** AO-3, **(D)** AO-4, **(E)** AO-5, **(F)** AO-6 stacking configurations for the AlN/Zr_2CO_2 heterostructure, the blue, yellow, cyan, black and red balls represent the Al, N, Zr, C, and O atoms, respectively.

2021b; Zhang et al., 2021b; Sun et al., 2021) and the modification of known 2D materials have become more and more exciting (Liu et al., 2019; Sun et al., 2019; Zhang et al., 2020c; Wang et al., 2021; Zheng et al., 2021). In many modification methods, two different materials are usually combined as a heterostructure by horizontal (Qin et al., 2019b; Ren et al., 2020a) or vertical direction [(Wang et al., 2020d), (Wang et al., 2020c)]. In particular, the vertical heterostructure is constructed by weak van der Waals (vdW) force at the interface instead of covalent bond, which can result tremendous and novel performances. For example, the type-II heterostructure possesses staggered band alignment, which has ability to separate the photogenerated electrons and holes, revealing a promising application as photocatalyst. It also has been proved by some theoretical and experimental investigations, such as TMDs/BP (Ren et al., 2019a), *h*-BN/C_2N (Wang et al., 2020e), TMDs/$Mg(OH)_2$ (Luo et al., 2019) etc. The type-I band structure in heterostructure can make the charge transfer from wide band gap materials to narrow band gap materials, which can be pretty reflected in light-emitting devices such as LEDs (Bellus et al., 2017; Ren et al., 2021b). Interestingly, the band structure of black/red phosphorus heterostructure can be transformed from type-I to Z-scheme system by quantum confinement effect (Shi et al., 2019). TMDs based heterostructure, such as $MoTe_2/WSe_2$, has excellent photoluminescence (about 1.1 eV from $MoTe_2$), which provides promising optoelectronic applications (Yamaoka et al., 2018). Furthermore, type-I heterostructure also can be used as a photocatalyst for water splitting because of remarkable light absorption characteristics (Do et al., 2020; Zhu et al., 2021a). More recently, 2D aluminum nitride (AlN) has attracted significant focus because of novel electronic (Zhang, 2012) and magnetic (Zhang and Zheng, 2011) performances, which also can be tuned by doping (Bai et al., 2015). Besides, some heterostructure constructed by AlN also have been studied, such as BiSb/AlN (Singh and Romero, 2017) and AlN/BP (Yang et al., 2017) etc. Importantly, it has been reported that the AlN films can be prepared on 6H–SiC substrates by various sputtering pressures by RF reactive magnetron sputtering (Kuang et al., 2012) and the AlN nanowires was also has been synthetized (Xu et al., 2003), which demonstrated the preparation method for AlN monolayer. At the same time, the Zr_2CO_2 as a MXene materials has been studied extensively to form vdW heterostructure (Zhu et al., 2021b). InSe/Zr_2CO_2 heterostructure possesses unique electron mobility (about 10^4 $cm^2/V{\cdot}s$) as a photocatalyst (He et al., 2019). MoS_2/Zr_2CO_2 heterostructure also has decent band edge positions for the redox reaction of the water splitting (Xu et al., 2020). Interestingly, Zr_2CO_2/blue phosphorene heterostructure has a transformable band structure between type-I and type-II under external strain (Guo et al., 2017). Moreover, the MXene also can be prepared by suitable means (Lei et al., 2015). Therefore, both AlN and MXene possess possibility of preparation, which also show the future synthetic work on AlN/MXene heterostructure. And the investigations about the heterostructure based on AlN and Zr_2CO_2 monolayer are rare, it is excited to explore the novel properties and the potential application of the AlN/Zr_2CO_2 heterostructure.

In this work, the AlN and Zr_2CO_2 are selected to build a heterostructure. Using first-principle theoretical calculation methods, the structural and electronic natures of the AlN/Zr_2CO_2 heterostructure are addressed, which shows that the

type-I band alignment in AlN/Zr_2CO_2 heterostructure gives a potential usage of light-emitting devices. Then, the interfacial performances of the heterostructure are calculated by charge density and potential drop. Finally, the light absorption capacity of the AlN/Zr_2CO_2 heterostructure is explored.

Computing Method

In this simulations work, the calculations were performed by first-principles method using density functional theory by the circumstances of Vienna ab initio simulation package (Kresse and Furthmüller, 1996a; Kresse and Furthmüller, 1996b; Capelle, 2006). The generalized gradient approximation and the projector augmented wave potentials were considered to explain the exchange correlation functional (Kresse and Joubert, 1999; Grimme, 2006). Besides, the DFT-D3 method was conducted using Grimme to demonstrate the weak disperson forces (Grimme et al., 2010). Furthermore, the Heyd–Scuseria–Ernzerhof hybrid method was used for decent electronic and optical results of the studied system (Heyd et al., 2005). Moreover, the energy cut-off was 500 eV. The Monkhorst–Pack *k*-point grids was 15 × 15 × 1 and the vacuum space was set as 25 Å, which can efficiently prevent the interaction of nearby layers. The convergence standard for force and energy were limited in 0.01 eV·$Å^{-1}$ and smaller than 0.01 meV, respectively.

RESULTS AND DISCUSSION

First, the AlN/Zr_2CO_2 is optimized by a decent lattice constant of 3.365 Å, which is comparable with of the AlN (3.127 Å) (Ren et al., 2020b) and Zr_2CO_2 (3.294 Å) (Guo et al., 2017) monolayers. When monolayered AlN and Zr_2CO_2 are combined to form the heterostructure, considering that there are various combination modes of AlN and Zr_2CO_2 monolayers, we only select the most representative highly symmetrical combination configurations among them. These six combination styles of AlN/Zr_2CO_2 heterostructure are shown as **Figures 1A–F**, named AO-1 to AO-6, respectively. For AO-1, the N and Al atoms are located on the upper O and upper Zr atoms, respectively. The AO-2 is obtained by putting the N and Al atoms on the C and lower O atoms, respectively. The AO-3 is built by locating the N and Al atoms on the C and lower Zr atoms, respectively. Then, fixing the N and Al atoms on the lower O and lower Zr atoms, respectively, can construct the AlN/Zr_2CO_2 heterostructure by AO-4 configuration. Differently, locating the N and Al atoms on the lower O and C atoms, respectively, can build the AO-5 configuration. Furthermore, AO-6 configuration is constructed by fixing the N and Al atoms on upper O and C atoms, respectively. Besides, the most stable stacking configuration of the AlN/Zr_2CO_2 heterostructure is decided by the binding energy, represented by E_b as follow:

$$E_b = E_{AlN/ZrCO2} - E_{AlN} - E_{Zr2CO2} \quad (1)$$

where $E_{AlN/Zr2CO2}$, E_{AlN} and E_{Zr2CO2} are showing the total energy of the AlN/Zr_2CO_2 system, original AlN and Zr_2CO_2 monolayers, respectively. Furthermore, the calculation demonstrations that the stacked structure in **Figure 1A** is the most stable heterostructure with binding energy of –36.05 meV/$Å^2$, which also proves that the single-layer AlN and Zr_2CO_2 are constructed by vdW force (Chen et al., 2013). In addition, the distance of interface and the bond length of these different stacking configurations of the optimized AlN/Zr_2CO_2 heterostructure are calculated in **Table 1**. Moreover, the following discussion in this work is based on the most stable stacking structure of AO-1.

The projected band energy of AlN/Zr_2CO_2 vdW heterostructure is obtained by HSE06 calculation, as shown in **Figure 2A**. One can clearly find that AlN/Zr_2CO_2 has a semiconductor nature with indirect band gap of 1.790 eV. In addition, the red and black marks are contributed from AlN and Zr_2CO_2 monolayers, respectively, suggesting that the (conduction band minimum) CBM and (the valence band maximum) VBM of AlN/Zr_2CO_2 vdW heterostructure are mainly resulted by Zr_2CO_2 monolayer. Thus, a type-I band structure is constructed in AlN/Zr_2CO_2 vdW heterostructure. Besides, the partial density of AlN/Zr_2CO_2 vdW heterostructure, as shown in **Figures 2B, 2is** also obtained to further prove the characteristics of intrinsic type-I band structure. It is obvious that the CBM and the VBM of the AlN/Zr_2CO_2 vdW heterostructure are mainly donated by Zr and O atoms, respectively.

TABLE 1 | The optimized distance of interface (*H*, Å) and the bond length (*L*, Å) of the AlN/Zr_2CO_2 heterostructure with different stacking styles.

	H	L_{Al-N}	L_{Zr-C}	L_{Zr-O}
AO-1	1.909	1.943	2.388	2.110
AO-2	2.231	1.945	2.373	2.139
AO-3	3.235	1.943	2.387	2.137
AO-4	3.626	1.943	2.387	2.136
AO-5	3.475	1.943	2.387	2.137
AO-6	2.710	1.943	2.387	2.131

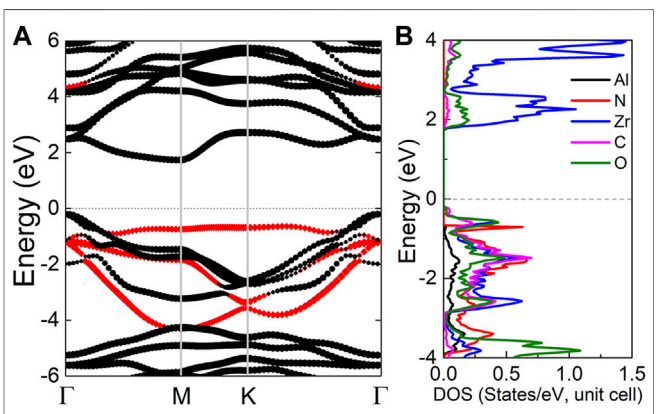

FIGURE 2 | (A) The projected band structure and **(B)** the partial density of states of the AlN/Zr_2CO_2 vdW heterostructure, the Fermi level is expressed by 0 shown as dash line.

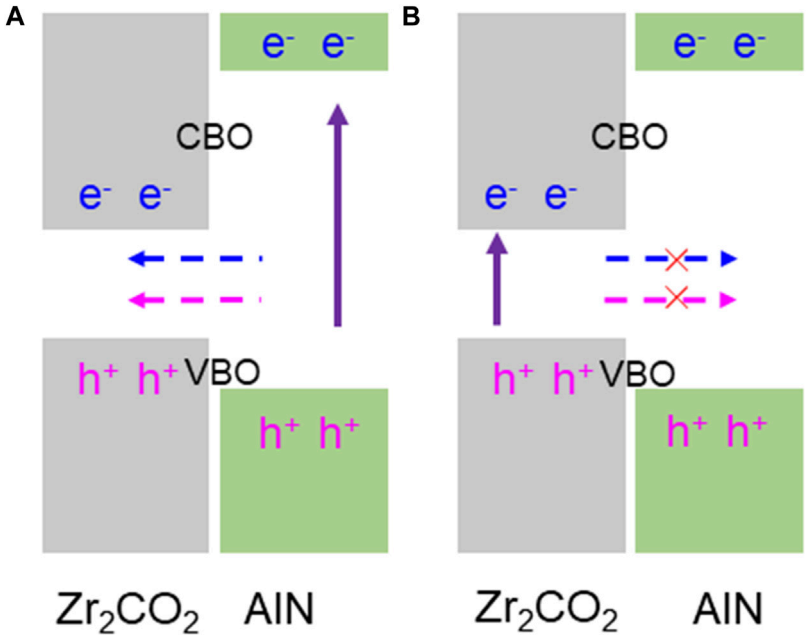

FIGURE 3 | Band alignment schematic of the excited charge transfer mode of the AlN/Zr_2CO_2 vdW heterostructure: **(A)** feasible and **(B)** limited charge migration mode.

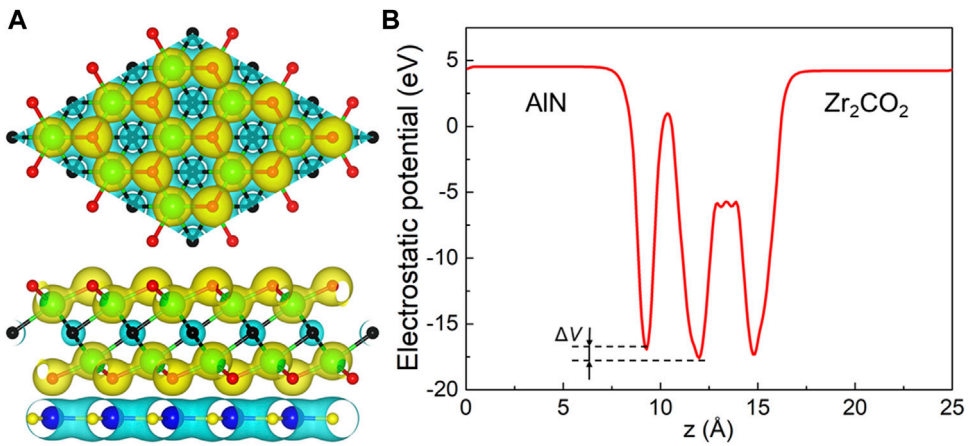

FIGURE 4 | (A) The charge density difference and the **(B)** potential drop of the AlN/Zr_2CO_2 vdW heterostructure. The yellow and cyan regions contribute the gaining and losing of electrons, respectively.

Such type-I band structure in the AlN/Zr_2CO_2 vdW heterostructure provides some important advanced applications in nano-devices. In AlN/Zr_2CO_2 vdW heterostructure, as shown in **Figure 3A**, CBM and VBM of AlN/Zr_2CO_2 vdW heterostructure are contributed by single-layer Zr_2CO_2, and the band gap of single-layer Zr_2CO_2 is less than that of single-layer AlN. When AlN/Zr_2CO_2 vdW heterostructure is excited by some external conditions, the electrons in the broad-band gap AlN monolayer are inspired and transferred to the CBM, generating holes at the VBM. It is worth noting that under the action of conduction band offset, CBO (valence band offset, VBO), electrons (holes) at the CBM (VBM) of the AlN layer can be transferred to the CBM (VBM) of the Zr_2CO_2 layer. Besides, the obtained CBO and VBO in AlN/Zr_2CO_2 vdW heterostructure are 2.432 and 0.471 eV respectively. While the electrons and holes excited in the relatively narrow-band gap of Zr_2CO_2 layer cannot be transferred to AlN layer due to low energy, in **Figure 3B**, which explains the AlN/Zr_2CO_2 vdW heterostructure can be considered as a potential light-emitting device material.

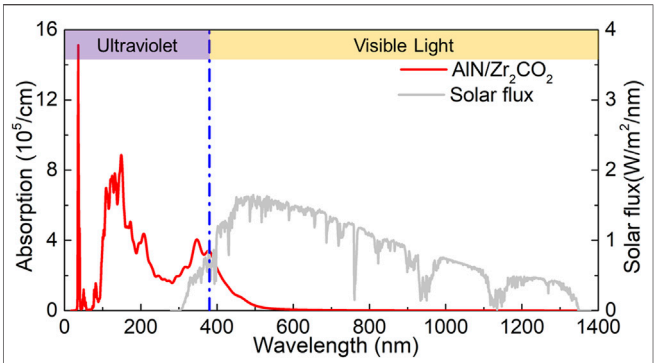

FIGURE 5 | The light absorption spectrum of the AlN/Zr_2CO_2 vdW heterostructure.

Then, we discussed the interface properties of AlN/Zr_2CO_2 vdW heterostructure by the charge density difference ($\Delta\rho$) and the potential drop (ΔV) in the interface. The charge density difference across the interface of the AlN/Zr_2CO_2 vdW heterostructure is calculated by:

$$\Delta\rho = \rho_{AlN/Zr2CO2} - \rho_{AlN} - \rho_{Zr2CO2}, \quad (2)$$

where $\rho_{AlN/Zr2CO2}$, ρ_{AlN} and ρ_{Zr2CO2} represent the charge density of the AlN/Zr_2CO_2 vdW heterostructure, monolayered AlN and Zr_2CO_2, respectively. Demonstrated by **Figure 4A**, the Zr_2CO_2 layer acts as an electron acceptor and AlN is an electron donor layer. Through Bader charge analysis (Tang et al., 2009), the obtained charge transfer from AlN layer to Zr_2CO_2 layer is 0.1603 $|e|$ in AlN/Zr_2CO_2 vdW heterostructure. Importantly, there is a certain degree of potential drop across the interface of the AlN/Zr_2CO_2 vdW heterostructure, shown as **Figure 4B**, and the calculated potential drop of 0.663 eV also play a critical role to assist the migration of the excited electrons and holes between the AlN/Zr_2CO_2 vdW heterostructure (Wang et al., 2018).

In order to produce more efficient light-emitting device, active materials should be able to effectively absorb light in the visible and near-infrared regions, especially type-I heterostructure. Therefore, we investigated the light absorption performance of AlN/Zr_2CO_2 vdW heterostructure by the calculation:

$$\alpha(\omega) = \frac{\sqrt{2}\omega}{c}\left\{\left[\varepsilon_1^2(\omega) + \varepsilon_2^2(\omega)\right]^{1/2} - \varepsilon_1(\omega)\right\}^{1/2}, \quad (3)$$

where ω is the angular frequency; α shows absorption coefficient and c is the speed of light. Besides, $\varepsilon_1(\omega)$ is used to explain the dielectric constant for real parts, which the imaginary one is demonstrated by $\varepsilon_2(\omega)$. As shown in **Figure 5** (the data source of solar flux is obtained from NREL website), AlN/Zr_2CO_2 vdW heterostructure demonstrates capacity to absorb sunlight over a wide range in the visible region the AlN/Zr_2CO_2 vdW heterostructure possesses a lot of absorption peaks. In ultraviolet region (left side of blue dotted line), the AlN/Zr_2CO_2 vdW heterostructure exhibits an absorption peak of $3.97 \times 10^5\ cm^{-1}$at the wavelength as 344 nm. In the in the visible region (right side of blue dotted line), the obtained absorption peak is $3.14 \times 10^5\ cm^{-1}$ locating at the wavelength of 369 nm, which is higher than other studied 2D heterostructures, such as WS_2/GeC ($2.651 \times 10^5\ cm^{-1}$) (Ren et al., 2021a), Arsenene/GaS ($1.403 \times 10^5\ cm^{-1}$) (Li et al., 2021), g-GaN/BSe ($1.470 \times 10^5\ cm^{-1}$) (Ren et al., 2019c) etc. The calculated results demonstrate the AlN/Zr_2CO_2 vdW heterostructure possesses excellent light absorption capacity.

CONCLUSION

In conclusion, the AlN and Zr_2CO_2 monolayers are constructed by vdW force to form a heterostructure. And the most stable AlN/Zr_2CO_2 is decided by the lowest binding energy of about −36.05 meV/Å^2. The, the HSE06 obtained projected band structure shows the AlN/Zr_2CO_2 vdW heterostructure possesses semiconductor nature with a band gap of 1.790 eV, and presents a type-I energy band alignment, which is a satisfaction candidate for light-emitting devices. Furthermore, the interface characteristics of AlN/Zr_2CO_2 vdW heterostructure is investigated by charge density difference (0.1603$|e|$ from AlN layer to Zr_2CO_2 layer) and potential drop (0.663 eV). Moreover, the AlN/Zr_2CO_2 vdW heterostructure explains a remarkable light absorption performance, which can further offer excellent technical guidance for nano light-emitting device materials.

DATA AVAILABILITY STATEMENT

The raw data supporting the conclusions of this article will be made available by the authors, without undue reservation.

AUTHOR CONTRIBUTIONS

All authors listed have made a substantial, direct, and intellectual contribution to the work and approved it for publication.

FUNDING

This investigation was supported by the Open Fund Project of Maanshan Engineering Technology, Research Center of Advanced Design for Automotive Stamping Dies (Grant number: QMSG202105).

ACKNOWLEDGMENTS

KR thanks the potential help by Xiaoqian Xu.

REFERENCES

Bai, Y., Deng, K., and Kan, E. (2015). Electronic and Magnetic Properties of an AlN Monolayer Doped with First-Row Elements: a First-Principles Study. *RSC Adv.* 5, 18352–18358. doi:10.1039/c4ra13522a

Bellus, M. Z., Li, M., Lane, S. D., Ceballos, F., Cui, Q., Zeng, X. C., et al. (2017). Type-I van der Waals heterostructure formed by MoS_2 and ReS_2 monolayers. *Nanoscale Horiz.* 2, 31–36. doi:10.1039/c6nh00144k

Capelle, K. (2006). A Bird's-Eye View of Density-Functional Theory. *Braz. J. Phys.* 36, 1318–1343. doi:10.1590/s0103-97332006000700035

Chen, M., Lu, Y., Wang, Z., Lan, H., Sun, G., and Ni, Z. (2021). Melt Pool Evolution on Inclined NV E690 Steel Plates during Laser Direct Metal Deposition. *Opt. Laser Techn.* 136, 106745. doi:10.1016/j.optlastec.2020.106745

Chen, X., Tian, F., Persson, C., Duan, W., and Chen, N.-x. (2013). Interlayer Interactions in Graphites. *Sci. Rep.* 3, 3046. doi:10.1038/srep03046

Ding, X.-Y., Zhang, C., Wang, D.-Q., Li, B.-S., Wang, Q., Yu, Z. G., et al. (2020). A New Carbon Allotrope:T_5-Carbon. *Scripta Materialia* 189, 72–77. doi:10.1016/j.scriptamat.2020.08.004

Do, T.-N., Idrees, M., Binh, N. T. T., Phuc, H. V., Hieu, N. N., Hoa, L. T., et al. (2020). Type-I band alignment of BX-ZnO (X = As, P) van der as high-efficiency water splitting photocatalysts: a first-principles study. *RSC Adv.* 10, 44545–44550. doi:10.1039/d0ra09701b

Geim, A. K., and Novoselov, K. S. (2007). The Rise of Graphene. *Nat. Mater* 6, 183–191. doi:10.1038/nmat1849

Grimme, S., Antony, J., Ehrlich, S., and Krieg, H. (2010). A Consistent and Accurate Ab Initio Parametrization of Density Functional Dispersion Correction (DFT-D) for the 94 Elements H-Pu. *J. Chem. Phys.* 132, 154104. doi:10.1063/1.3382344

Grimme, S. (2006). Semiempirical GGA-type Density Functional Constructed with a Long-Range Dispersion Correction. *J. Comput. Chem.* 27, 1787–1799. doi:10.1002/jcc.20495

Guo, Z., Miao, N., Zhou, J., Sa, B., and Sun, Z. (2017). Strain-mediated type-I/type-II transition in MXene/Blue phosphorene van der Waals heterostructures for flexible optical/electronic devices. *J. Mater. Chem. C* 5, 978–984. doi:10.1039/c6tc04349f

He, Y., Zhang, M., Shi, J.-j., Cen, Y.-l., and Wu, M. (2019). Improvement of Visible-Light Photocatalytic Efficiency in a Novel InSe/Zr_2CO_2 Heterostructure for Overall Water Splitting. *J. Phys. Chem. C* 123, 12781–12790. doi:10.1021/acs.jpcc.9b01175

Heyd, J., Peralta, J. E., Scuseria, G. E., and Martin, R. L. (2005). Energy Band Gaps and Lattice Parameters Evaluated with the Heyd-Scuseria-Ernzerhof Screened Hybrid Functional. *J. Chem. Phys.* 123, 174101. doi:10.1063/1.2085170

Kamal, C., and Ezawa, M. (2015). Arsenene: Two-Dimensional Buckled and Puckered Honeycomb Arsenic Systems. *Phys. Rev. B* 91, 085423. doi:10.1103/physrevb.91.085423

Kresse, G., and Furthmüller, J. (1996). Efficiency of Ab-Initio Total Energy Calculations for Metals and Semiconductors Using a Plane-Wave Basis Set. *Comput. Mater. Sci.* 6, 15–50. doi:10.1016/0927-0256(96)00008-0

Kresse, G., and Furthmüller, J. (1996). Efficient Iterative Schemes Forab Initiototal-Energy Calculations Using a Plane-Wave Basis Set. *Phys. Rev. B* 54, 11169–11186. doi:10.1103/physrevb.54.11169

Kresse, G., and Joubert, D. (1999). From Ultrasoft Pseudopotentials to the Projector Augmented-Wave Method. *Phys. Rev. B* 59, 1758–1775. doi:10.1103/physrevb.59.1758

Kuang, X.-P., Zhang, H.-Y., Wang, G.-G., Cui, L., Zhu, C., Jin, L., et al. (2012). AlN Films Prepared on 6H-SiC Substrates under Various Sputtering Pressures by RF Reactive Magnetron Sputtering. *Appl. Surf. Sci.* 263, 62–68. doi:10.1016/j.apsusc.2012.08.121

Lei, J.-C., Zhang, X., and Zhou, Z. (2015). Recent Advances in MXene: Preparation, Properties, and Applications. *Front. Phys.* 10, 276–286. doi:10.1007/s11467-015-0493-x

Li, J., Huang, Z., Ke, W., Yu, J., Ren, K., and Dong, Z. (2021). High solar-to-hydrogen efficiency in Arsenene/GaX (X = S, Se) van der Waals heterostructure for photocatalytic water splitting. *J. Alloy. Compound.* 866. doi:10.1016/j.jallcom.2021.158774

Li, L., Yu, Y., Ye, G. J., Ge, Q., Ou, X., Wu, H., et al. (2014). Black Phosphorus Field-Effect Transistors. *Nat. Nanotech* 9, 372–377. doi:10.1038/nnano.2014.35

Liu, X., Zhang, Z., Luo, Z., Lv, B., and Ding, Z. (2019). Tunable Electronic Properties of Graphene/g-AlN Heterostructure: The Effect of Vacancy and Strain Engineering. *Nanomaterials* 9, 1674. doi:10.3390/nano9121674

Lou, J., Ren, K., Huang, Z., Huo, W., Zhu, Z., and Yu, J. (2021). Electronic and Optical Properties of Two-Dimensional Heterostructures Based on Janus XSSe (X = Mo, W) and $Mg(OH)_2$: a First Principles Investigation. *RSC Adv.* 11, 29576–29584. doi:10.1039/d1ra05521f

Luo, Y., Wang, S., Ren, K., Chou, J.-P., Yu, J., Sun, Z., et al. (2019). Transition-metal dichalcogenides/$Mg(OH)_2$ van der Waals heterostructures as promising water-splitting photocatalysts: a first-principles study. *Phys. Chem. Chem. Phys.* 21, 1791–1796. doi:10.1039/c8cp06960c

Pi, L., Li, L., Liu, K., Zhang, Q., Li, H., and Zhai, T. (2019). Recent Progress on 2D Noble-Transition-Metal Dichalcogenides. *Adv. Funct. Mater.* 29, 1904932. doi:10.1002/adfm.201904932

Pumera, M., and Sofer, Z. (2017). 2D Monoelemental Arsenene, Antimonene, and Bismuthene: Beyond Black Phosphorus. *Adv. Mater.* 29, 1605299. doi:10.1002/adma.201605299

Qi, K., Xing, X., Zada, A., Li, M., Wang, Q., Liu, S.-y., et al. (2020). Transition Metal Doped ZnO Nanoparticles with Enhanced Photocatalytic and Antibacterial Performances: Experimental and DFT Studies. *Ceramics Int.* 46, 1494–1502. doi:10.1016/j.ceramint.2019.09.116

Qin, H., and Liu, Y. (2017). Interlayer Shear Behaviors of Graphene-Carbon Nanotube Network. *J. Appl. Phys.* 122, 125108. doi:10.1063/1.4992025

Qin, H., Pei, Q.-X., Liu, Y., and Zhang, Y.-W. (2019). The Mechanical and thermal Properties of MoS_2-WSe_2 Lateral Heterostructures. *Phys. Chem. Chem. Phys.* 21, 15845–15853. doi:10.1039/c9cp02499a

Qin, H., Pei, Q.-X., Liu, Y., and Zhang, Y.-W. (2019). Thermal Transport in Graphene-Based Layered Materials: An Analytical Model Validated with Extensive Molecular Dynamics Simulations. *Carbon* 155, 114–121. doi:10.1016/j.carbon.2019.08.062

Ren, K., Liu, X., Chen, S., Cheng, Y., Tang, W., and Zhang, G. (2020). Remarkable Reduction of Interfacial Thermal Resistance in Nanophononic Heterostructures. *Adv. Funct. Mater.* 30, 2004003. doi:10.1002/adfm.202004003

Ren, K., Luo, Y., Wang, S., Chou, J.-P., Yu, J., Tang, W., et al. (2019). A van der Waals Heterostructure Based on Graphene-like Gallium Nitride and Boron Selenide: A High-Efficiency Photocatalyst for Water Splitting. *ACS Omega* 4, 21689–21697. doi:10.1021/acsomega.9b02143

Ren, K., Shu, H., Huo, W., Cui, Z., Yu, J., and Xu, Y. (2021a). Mechanical, Electronic and Optical Properties of Novel B_2P_6 Monolayer: Ultrahigh Carrier Mobility and Strong Optical Absorption. *Phys. Chem. Chem. Phys.*. doi:10.1039/D1CP03838A

Ren, K., Sun, M., Luo, Y., Wang, S., Yu, J., and Tang, W. (2019). First-principle Study of Electronic and Optical Properties of Two-Dimensional Materials-Based Heterostructures Based on Transition Metal Dichalcogenides and boron Phosphide. *Appl. Surf. Sci.* 476, 70–75. doi:10.1016/j.apsusc.2019.01.005

Ren, K., Wang, S., Luo, Y., Chou, J.-P., Yu, J., Tang, W., et al. (2020). High-efficiency photocatalyst for water splitting: a Janus MoSSe/XN (X = Ga, Al) van der Waals heterostructure. *J. Phys. D: Appl. Phys.* 53, 185504. doi:10.1088/1361-6463/ab71ad

Ren, K., Zheng, R., Xu, P., Cheng, D., Huo, W., Yu, J., et al. (2021b). Electronic and Optical Properties of Atomic-Scale Heterostructure Based on MXene and MN (M = Al, Ga): A DFT Investigation. *Nanomaterials* 11, 2236. doi:10.3390/nano11092236

Shi, R., Liu, F., Wang, Z., Weng, Y., and Chen, Y. (2019). Black/red Phosphorus Quantum Dots for Photocatalytic Water Splitting: from a Type I Heterostructure to a Z-Scheme System. *Chem. Commun.* 55, 12531–12534. doi:10.1039/c9cc06146k

Singh, S., and Romero, A. H. (2017). Giant Tunable Rashba Spin Splitting in a Two-Dimensional BiSb Monolayer and in BiSb/AlN Heterostructures. *Phys. Rev. B* 95, 165444. doi:10.1103/physrevb.95.165444

Sun, M., Chou, J.-P., Hu, A., and Schwingenschlögl, U. (2019). Point Defects in Blue Phosphorene. *Chem. Mater.* 31, 8129–8135. doi:10.1021/acs.chemmater.9b02871

Sun, M., Luo, Y., Yan, Y., and Schwingenschlögl, U. (2021). Ultrahigh Carrier Mobility in the Two-Dimensional Semiconductors B8Si4, B8Ge4, and B8Sn4. *Chem. Mater.* 33, 6475–6483. doi:10.1021/acs.chemmater.1c01824

Sun, M., and Schwingenschlögl, U. (2020). B_2P_6: A Two-Dimensional Anisotropic Janus Material with Potential in Photocatalytic Water Splitting and Metal-Ion Batteries. *Chem. Mater.* 32, 4795–4800. doi:10.1021/acs.chemmater.0c01536

Sun, M., and Schwingenschlögl, U. (2021). Structure Prototype Outperforming MXenes in Stability and Performance in Metal-Ion Batteries: A High Throughput Study. *Adv. Energ. Mater.* 11, 2003633. doi:10.1002/aenm.202003633

Sun, M., and Schwingenschlögl, U. (2021). Unique Omnidirectional Negative Poisson's Ratio in δ-Phase Carbon Monochalcogenides. *J. Phys. Chem. C* 125, 4133–4138. doi:10.1021/acs.jpcc.0c11555

Sun, M., Schwingenschlögl, U., and δ-, C. S. (2020). A Direct-Band-Gap Semiconductor Combining Auxeticity, Ferroelasticity, and Potential for High-Efficiency Solar Cells. *Phys. Rev. Appl.* 14, 044015. doi:10.1103/physrevapplied.14.044015

Sun, M., Yan, Y., and Schwingenschlögl, U. (2020). Beryllene: A Promising Anode Material for Na- and K-Ion Batteries with Ultrafast Charge/Discharge and High Specific Capacity. *J. Phys. Chem. Lett.* 11, 9051–9056. doi:10.1021/acs.jpclett.0c02426

Tan, Z.-L., Wei, J.-X., Liu, Y., Rehman, W., Hou, L.-R., and Yuan, C.-Z. (2021). V_2CT_x MXene and its Derivatives: Synthesis and Recent Progress in Electrochemical Energy Storage Applications. *Rare Met.*, 1–23.

Tang, W., Sanville, E., and Henkelman, G. (2009). A Grid-Based Bader Analysis Algorithm without Lattice Bias. *J. Phys. Condens. Matter* 21, 084204. doi:10.1088/0953-8984/21/8/084204

Wang, B., Wang, X., Wang, P., Yang, T., Yuan, H., Wang, G., et al. (2019). Bilayer $MoSe_2/HfS_2$ Nanocomposite as a Potential Visible-Light-Driven Z-Scheme Photocatalyst. *Nanomaterials* 9, 1706. doi:10.3390/nano9121706

Wang, G., Gong, L., Li, Z., Wang, B., Zhang, W., Yuan, B., et al. (2020). A Two-Dimensional CdO/CdS Heterostructure Used for Visible Light Photocatalysis. *Phys. Chem. Chem. Phys.* 22, 9587–9592. doi:10.1039/d0cp00876a

Wang, G., Li, Z., Wu, W., Guo, H., Chen, C., Yuan, H., et al. (2020). A Two-Dimensional h-BN/C_2N Heterostructure as a Promising Metal-free Photocatalyst for Overall Water-Splitting. *Phys. Chem. Chem. Phys.* 22, 24446–24454. doi:10.1039/d0cp03925j

Wang, G., Tang, W., Geng, L., Li, Y., Wang, B., Chang, J., et al. (2020). Rotation Tunable Photocatalytic Properties of ZnO/GaN Heterostructures. *Phys. Status Solidi B* 257, 1900663. doi:10.1002/pssb.201900663

Wang, G., Zhang, L., Li, Y., Zhao, W., Kuang, A., Li, Y., et al. (2020). Biaxial Strain Tunable Photocatalytic Properties of 2D ZnO/GeC Heterostructure. *J. Phys. D: Appl. Phys.* 53, 015104. doi:10.1088/1361-6463/ab440e

Wang, K., Ren, K., Cheng, Y., Zhang, M., Wang, H., and Zhang, G. (2020). Effects of Molecular Adsorption on the Spin-Wave Spectrum and Magnon Relaxation in Two-Dimensional $Cr_2Ge_2Te_6$. *Phys. Chem. Chem. Phys.* 22, 22047–22054. doi:10.1039/d0cp03884a

Wang, S., Tian, H., Ren, C., Yu, J., and Sun, M. (2018). Electronic and Optical Properties of Heterostructures Based on Transition Metal Dichalcogenides and Graphene-like Zinc Oxide. *Sci. Rep.* 8, 12009. doi:10.1038/s41598-018-30614-3

Wang, Z., Zhang, Z., Liu, S., Shao, C., Robertson, J., and Guo, Y. (2021). Impact of Carbon-Carbon Defects at the SiO2/4H-SiC (0001) Interface: a First-Principles Calculation. *J. Phys. D: Appl. Phys.* 55, 025109. doi:10.1088/1361-6463/ac2bc9

Xie, G., Shen, Y., Wei, X., Yang, L., Xiao, H., Zhong, J., et al. (2014). A Bond-Order Theory on the Phonon Scattering by Vacancies in Two-Dimensional Materials. *Sci. Rep.* 4, 5085. doi:10.1038/srep05085

Xu, C., Xue, L., Yin, C., and Wang, G. (2003). Formation and Photoluminescence Properties of AlN Nanowires. *Phys. Stat. Sol. (A)* 198, 329–335. doi:10.1002/pssa.200306612

Xu, X., Ge, X., Liu, X., Li, L., Fu, K., Dong, Y., et al. (2020). Two-dimensional M_2CO_2/MoS_2 (M = Ti, Zr and Hf) van der Waals heterostructures for overall water splitting: A density functional theory study. *Ceramics Int.* 46, 13377–13384. doi:10.1016/j.ceramint.2020.02.119

Yamaoka, T., Lim, H. E., Koirala, S., Wang, X., Shinokita, K., Maruyama, M., et al. (2018). Efficient Photocarrier Transfer and Effective Photoluminescence Enhancement in Type I Monolayer $MoTe_2/WSe_2$ Heterostructure. *Adv. Funct. Mater.* 28, 1801021. doi:10.1002/adfm.201801021

Yang, Q., Tan, C.-J., Meng, R.-S., Jiang, J.-K., Liang, Q.-H., Sun, X., et al. (2017). AlN/BP Heterostructure Photocatalyst for Water Splitting. *IEEE Electron. Device Lett.* 38, 145–148. doi:10.1109/led.2016.2633487

Zhang, C.-w. (2012). First-principles Study on Electronic Structures and Magnetic Properties of AlN Nanosheets and Nanoribbons. *J. Appl. Phys.* 111, 043702. doi:10.1063/1.3686144

Zhang, C.-w., and Zheng, F.-b. (2011). First-principles Prediction on Electronic and Magnetic Properties of Hydrogenated AlN Nanosheets. *J. Comput. Chem.* 32, 3122–3128. doi:10.1002/jcc.21902

Zhang, C., Cao, Y., Liu, Y., Hu, H.-J., Yu, Z. G., and Zhang, Y.-W. (2021). Bct-C_5: A New Body-Centered Tetragonal Carbon Allotrope. *Diamond Relat. Mater.* 119, 108571. doi:10.1016/j.diamond.2021.108571

Zhang, C., Zhou, H., Chen, S., Zhang, G., Yu, Z. G., Chi, D., et al. (2021). Recent Progress on 2D Materials-Based Artificial Synapses. *Crit. Rev. Solid State. Mater. Sci.*, 1–26. doi:10.1080/10408436.2021.1935212

Zhang, Z., Guo, Y., and Robertson, J. (2020). Origin of Weaker Fermi Level Pinning and Localized Interface States at Metal Silicide Schottky Barriers. *J. Phys. Chem. C* 124. doi:10.1021/acs.jpcc.0c06228

Zhang, Z., Guo, Y., and Robertson, J. (2020). Termination-dependence of Fermi Level Pinning at Rare-Earth arsenide/GaAs Interfaces. *Appl. Phys. Lett.* 116, 251602. doi:10.1063/5.0007479

Zhang, Z., Huang, B., Qian, Q., Gao, Z., Tang, X., and Li, B. (2020). Strain-tunable III-nitride/ZnO Heterostructures for Photocatalytic Water-Splitting: A Hybrid Functional Calculation. *APL Mater.* 8, 041114. doi:10.1063/5.0005648

Zheng, Z., Ren, K., Huang, Z., Zhu, Z., Wang, K., Shen, Z., et al. (2021). Remarkably Improved Curie Temperature for Two-Dimensional CrI_3 by Gas Molecular Adsorption: a DFT Study. *Semicond. Sci. Tech.* 36 (7), 075015. doi:10.1088/1361-6641/ac01a2

Zhu, X. T., Xu, Y., Cao, Y., Zhao, Y. Q., Sheng, W., Nie, G.-Z., et al. (2021). Investigation of the Electronic Structure of Two-Dimensional GaN/Zr_2CO_2 hetero-junction: Type-II Band Alignment with Tunable Bandgap. *Appl. Surf. Sci.* 542, 148505. doi:10.1016/j.apsusc.2020.148505

Zhu, Z., Ren, K., Shu, H., Cui, Z., Huang, Z., Yu, J., et al. (2021). First-Principles Study of Electronic and Optical Properties of Two-Dimensional WSSe/BSe van der Waals Heterostructure with High Solar-to-Hydrogen Efficiency. *Catalysts* 11, 991. doi:10.3390/catal11080991

Conflict of Interest: The authors declare that the research was conducted in the absence of any commercial or financial relationships that could be construed as a potential conflict of interest.